the applied modulator bias (the bias increases towards the left) and the vertical axis is the polarisation-resolved output power. The modulator is driven at 500 Hz with a sawtooth waveform (800 V_{pp}). Figs. 3*a* and *b* show the TE and TM modes, respectively. In the case that the bias voltage is small, the TE mode is dominant and all the output power is TE-polarised. Further increase of the bias voltage causes the loss in the TE cavity to increase and results in a transition from the TE to the TM polarisation. The transition is sharp and clean.

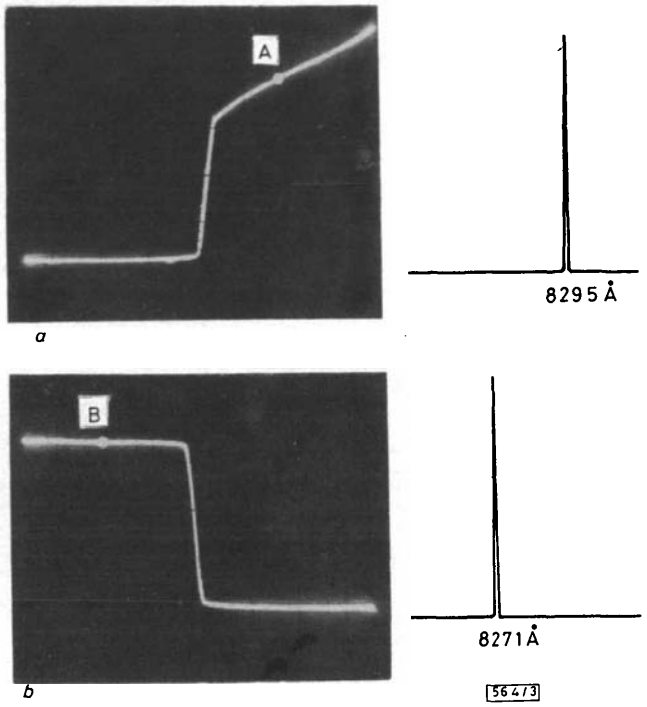

Fig. 3 *Polarisation-resolved optical output power (vertical axis) against modulator bias voltage (horizontal axis)*

Modulator bias voltage increases towards the left. Optical spectra are also shown

A remarkable feature of this polarisation switching is the improvement in the temporal coherence of the two states. Optical spectra corresponding to the points indicated as A and B are also shown in Fig. 3. Single-longitudinal-mode oscillation with a side-mode suppression ratio of 30 dB was measured by the monochromator and no external-cavity side modes are observed in the scanning Fabry–Perot interferometer display. It is to be noted that these single-frequency oscillations are very stable because strong optical feedback is utilised, and the linewidth is expected to be in the order of 10 kHz.[7]

To the best of our knowledge, polarisation switching in semiconductor lasers reported so far has always displayed multilongitudinal-mode oscillation with correspondingly low temporal coherence.[4,5] A polarisation-selective external-cavity laser is an effective way to have TE to TM switching with a high degree of temporal coherence. It should be noted that polarisation bistability has been observed in this configuration,† but the conditions for switching between single modes and bistability are different and will be reported elsewhere.

In conclusion, we have demonstrated single-frequency polarisation switching in an external-cavity semiconductor laser. A novel T-shaped polarisation-selective external-cavity laser with an intracavity electro-optic modulator allows electrically controlled switching between the TE and TM modes. The temporal coherence properties are greatly improved over other schemes of polarisation switching.

T. FUJITA* *16th June 1987*
A. SCHREMER
C. L. TANG

School of Electrical Engineering
Cornell University
Ithaca, NY 14853, USA

* On leave from Optoelectronics Laboratory, Semiconductor Research Center, Matsushita Electric Industrial Company Ltd., Osaka, Japan

References

1 IKEGAMI, T.: 'Reflectivity of mode at facet and oscillation mode in double-heterostructure injection lasers', *IEEE J. Quantum Electron.*, 1972, **QE-8**, pp. 470–476
2 PATEL, N. B., RIPPER, J. E., and BROSSON, P.: 'Behavior of threshold current and polarization of stimulated emission of GaAs injection lasers under uniaxial stress', *ibid.*, 1973, **QE-9**, pp. 338–341
3 CHEN, Y. C., and LIU, J. M.: 'Direct polarization switching in semiconductor lasers', *Appl. Phys. Lett.*, 1984, **45**, pp. 604–606
4 MORI, Y., SHIBATA, J., and KAJIWARA, T.: 'Picosecond-switching optical bistability in a TM-wave injected BH laser'. 18th conference on solid-state devices and materials, Tokyo, 1986, Extended abstracts, pp. 723–724
5 SAPIA, A., SPANO, P., and DAINO, B.: 'Polarization switching in semiconductor lasers driven via injection from an external radiation', *Appl. Phys. Lett.*, 1987, **50**, pp. 57–59
6 SATO, H., FUJITA, T., and OHYA, J.: 'Theoretical analysis of longitudinal mode coupling in external cavity semiconductor lasers', *IEEE J. Quantum Electron.*, 1985, **QE-21**, pp. 284–291
7 SATO, H., and OHYA, J.: 'Theory of spectral linewidth of external cavity semiconductor lasers', *ibid.*, 1986, **QE-22**, pp. 1060–1063

† FUJITA, T., SCHREMER, A., and TANG, C. L.: submitted for publication

FERRITE TUNABLE METAL INSERT FILTER

Indexing terms: Microwave devices and components, Waveguide components, Ferrite devices, Microwave filters

A novel type of magnetically tunable waveguide filter is presented which is highly appropriate for *E*-plane integrated circuit applications. The design theory, which is based on the field expansion into normalised eigenmodes and the modal *S*-matrix description of the discontinuities, includes both higher-order mode interaction and finite thickness of the *E*-plane metal, as well as of the lateral ferrite inserts. Optimised design data for two- and three-resonator-type filters are given for midband frequencies of about 15·3–15·4 GHz and 14·1–14·8 GHz. The theory is verified by measurements.

Introduction: Magnetically tunable bandpass filters[1–3] are of considerable importance, for example for use as receiver preselectors. Well known techniques include ferrimagnetic YIG[1] resonators or ferrite-slab-loaded evanescent-mode waveguide filters.[2,3] This letter introduces a new type of magnetically tunable filter (Fig. 1) which is based on *E*-plane metal-insert structures[4–6] with lateral ferrite slabs in the waveguide sections; the centre frequency is controlled by the DC magnetic field. The design combines the advantages inherent in the single components: the low-cost, low-loss metal-etching fabrication techniques applicable for the metal inserts, and the power-handling capability of the lateral ferrite slab structure. Moreover, the filter type is highly appropriate for millimetre-wave integrated circuit designs.

Theory: The method for the computer optimisation for the magnetically tunable filters, which is based on field expansion into normalised incident and scattered waves,[6,7] meets the requirement of taking into account the higher-order mode coupling effects at all discontinuities, and yields directly the overall scattering matrix along the filter structure. The structure is decomposed into two key building block discontinuities: waveguide-to-waveguide with lateral ferrite slabs, and waveguide-to-waveguide separated by the metal insert with additional lateral ferrite slabs (Fig. 1). Combination with the known scattering matrices of the corresponding intermediate homogeneous waveguide sections yields the total scattering matrix of the filter element. The overall scattering matrix of the total filter is calculated by a suitable direct combination of all single modal scattering matrices,[6,7,10,11] the lengths of the intermediate homogeneous rectangular waveguide sections being reduced to zero if ferrite slab-loaded structures are joined together directly.

The field

$$\nabla \times \vec{H} = j\omega\varepsilon\vec{E} \qquad \nabla \cdot (\langle\tilde{\mu}\rangle\vec{H}) = 0$$
$$\nabla \times \vec{E} = -j\omega\langle\tilde{\mu}\rangle\vec{H} \qquad \nabla \cdot \vec{E} = 0 \tag{1}$$

in the homogeneous subregions (Fig. 1) is derived from suitably defined electric and magnetic field components, e.g. $e_{1,2} \cdot \vec{e}_y$ and $h_{1,2} \cdot \vec{e}_x$ respectively, which may be expressed as a sum of N eigenmodes[6,7] satisfying the vector Helmholtz equation and the boundary conditions at the metallic sidewalls. For example, for 1 (I) and 2 (II), the lower and upper regions separated by the metal insert (Fig. 1) of finite thickness $d - c$, respectively, the relations are

$$e_{1n} = \begin{cases} E^{I}_{1n} \sin (k^{I}_{Fn}(x)) & x \in (0, w) \\ E^{I}_{2n} \sin (k^{I}_{Ln}(c - x)) & x \in (w, c) \end{cases}$$
$$e_{2n} = \begin{cases} E^{II}_{1n} \sin (k^{II}_{Ln}(x - d)) & x \in (d; a - w) \\ E^{II}_{2n} \sin (k^{II}_{Fn}(a - x)) & x \in (a - w, a) \end{cases} \tag{2a}$$

$$h_{1n} = \begin{cases} \dfrac{j\gamma_n}{\omega\mu_0\mu_{ef}} E^{I}_{1n} \sin (k^{I}_{Fn}(x)) \\ \quad - \dfrac{E^{I}_{1n}\left(\dfrac{\kappa}{\mu}\right)k^{I}_{Fn}}{\omega\mu_0\mu_{ef}} \cos (k^{I}_{Fn}(x)) & x \in (O, w) \\ \dfrac{j\gamma_n}{\omega\mu_0} E^{I}_{2n} \sin (k^{I}_{Ln}(c - x)) & x \in (w, c) \end{cases} \tag{2b}$$

$$h_{2n} = \begin{cases} \dfrac{j\gamma_n}{\omega\mu_0} E^{II}_{1n} \sin (k^{II}_{Ln}(x - d)) & x \in (d, a - w) \\ \dfrac{j\gamma_n E^{II}_{2n}}{\omega\mu_0\mu_{ef}} \sin (k^{II}_{Fn}(a - x)) \\ \quad + \dfrac{E^{II}_{2n}\left(\dfrac{\kappa}{\mu}\right)k^{II}_{Fn}}{\omega\mu_0\mu_{ef}} \cos (k^{II}_{Fn}(a - x)) & x \in (a - w, a) \end{cases}$$

where k_F and k_L are the wavenumbers in the related ferrite-filled or empty regions, and a z-dependence of exp $(-\gamma_n z)$ is understood. For a DC magnetic field in the y-direction the permeability tensor takes the form given in References 9 and 10. The propagation factors γ_n are determined numerically via field matching[10,11] along the ferrite slab boundaries.

For calculating the modal scattering matrix S of the step discontinuities, the related biorthogonality relations[8] for anisotropic structures have to be taken into account. Matching of the transversal field components yields the relation between the still unknown amplitude coefficients through

$$(B) = (S)(A) \tag{3}$$

with the wave amplitude vectors A and B of the incident and reflected waves, respectively.

For computer optimisation[6,7,9] the expansion into 10 eigenmodes at each discontinuity has turned out to yield sufficient convergence behaviour. The final design data are proven through an expansion into 30 eigenmodes.

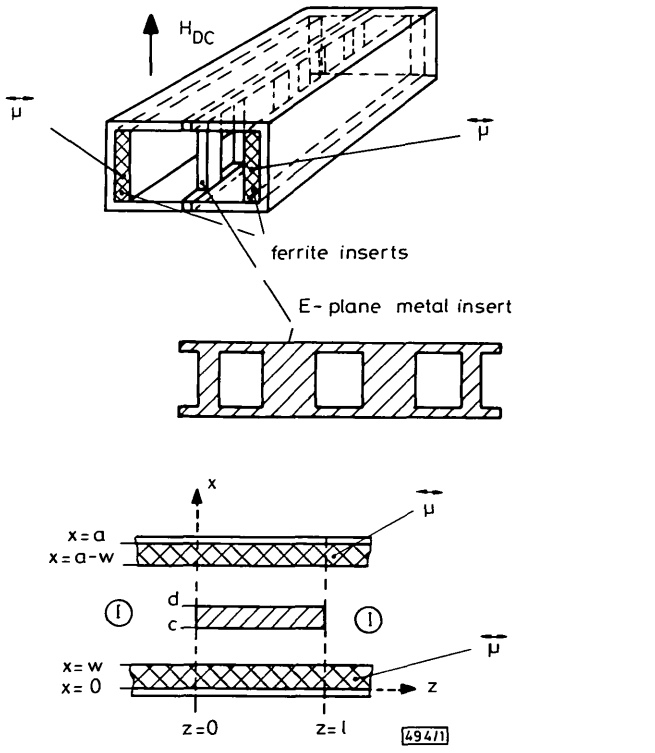

Fig. 1 *Metal insert filter with additional lateral ferrite slabs of width w for magnetic tuning of midband frequency by alternating magnetic DC field strength H_{DC}*

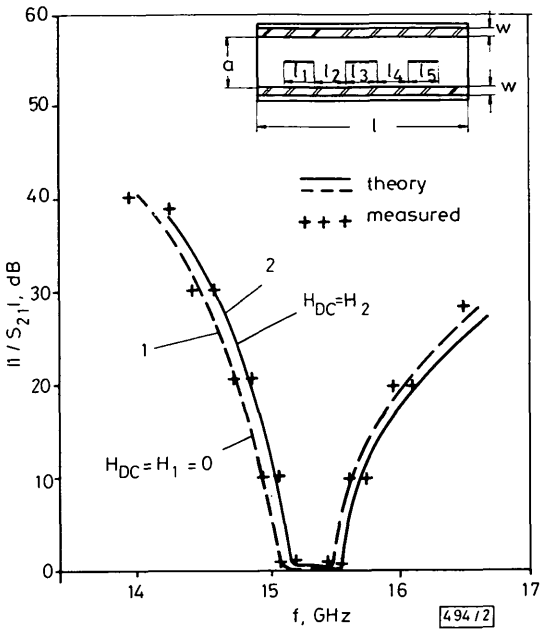

Fig. 2 *Filter response of a two-resonator metal insert filter with lateral ferrite TTVG-1200 slabs of width w = 0·5 mm, at two different DC field strengths*

Filter dimensions $a = 15{\cdot}799$ mm, $b = a/2$, $l_1 = l_5 = 3{\cdot}263$ mm, $l_2 = l_4 = 8{\cdot}914$ mm, $l_3 = 8{\cdot}578$ mm, metal insert thickness $t = 0{\cdot}19$ mm; length of ferrite slab $l = 37{\cdot}5$ mm
DC field strengths: $H_1 = 0$, $H_2 = 1{\cdot}72 \times 10^5$ A/m

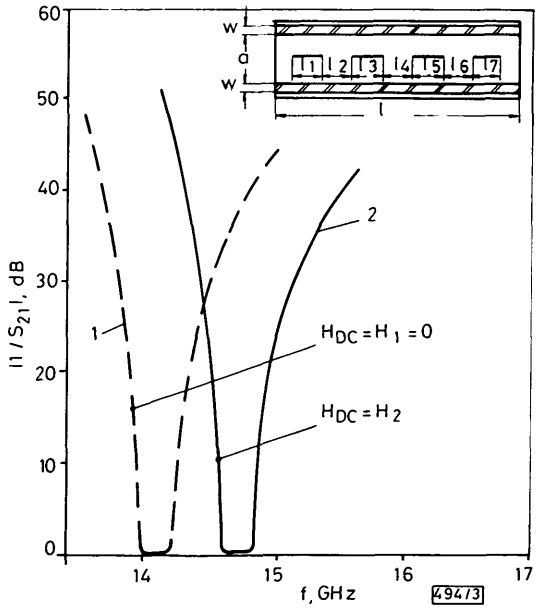

Fig. 3 *Filter response of a three-resonator metal insert filter with lateral ferrite RF-8 slabs of width = 1 mm, at two different DC field strengths*

Filter dimensions: $a = 15{\cdot}799$ mm, $b = a/2$, $l_1 = l_7 = 3{\cdot}590$ mm, $l_2 = l_6 = 8{\cdot}916$ mm, $l_3 = l_5 = 9{\cdot}417$ mm, $l_4 = 8{\cdot}921$ mm, metal insert thickness $t = 0{\cdot}19$ mm
DC field strengths: $H_1 = 0$, $H_2 = 8 \times 10^4$ A/m

Results: A computer-optimised, two-resonator, magnetically tunable, metal insert filter with lateral ferrite TTVG-1200 slabs of width 0·5 mm has been chosen for a first design example (Fig. 2). The tuning bandwidth of the filter may be improved by introducing lateral ferrite slabs of increased width (see Fig. 3), where the result of an optimised three-resonator Ku-band filter is indicated, with lateral ferrite RF-8 slabs of width $w = 1$ mm. As all relevant parameters are included in the design theory, the measured filter characteristic agrees well with the theoretically predicted values (Fig. 2).

Acknowledgment: The authors thank the German Research Society DFG for financial support under contract no. Ar 138/6-1.

J. UHER
J. BORNEMANN
F. ARNDT

Microwave Department
University of Bremen
Kufsteiner Strasse NW1
D-2800 Bremen 33, W. Germany

5th June 1987

References

1 MATTHAEI, G. L., YOUNG, L., and JONES, E. M. T.: 'Microwave filters, impedance-matching networks, and coupling structures' (McGraw-Hill, New York, 1964), Chap. 17
2 SKEDD, R. F., and CRAVEN, G.: 'Magnetically tunable multisection bandpass filters in ferrite-loaded evanescent waveguide', *Electron. Lett.*, 1967, **3**, pp. 62–63
3 SNYDER, R. V.: 'Stepped-ferrite tunable evanescent filters', *IEEE Trans.*, 1981, **MTT-29**, pp. 364–371
4 MEIER, P. J.: 'Integrated fin-line millimeter components', *ibid.*, 1974, **MTT-22**, pp. 1209–1216
5 KONISHI, Y., and UENAKADA, K.: 'The design of a bandpass filter with inductive strip—planar circuit mounted in waveguide', *ibid.*, 1979, **MTT-22**, pp. 869–873
6 VAHLDIEK, R., BORNEMANN, J., ARNDT, F., and GRAUERHOL, D.: 'Optimized waveguide *E*-plane metal insert filters for millimeter-wave applications', *ibid.*, 1983, **MTT-31**, pp. 65–69
7 ARNDT, F., BORNEMANN, J., HECKMANN, D., PIONTEK, C., SEMMEROW, H., and SCHUELER, H.: 'Modal S-matrix method for the optimum design of inductively direct-coupled cavity filters', *IEE Proc. H, Microwaves, Antennas & Propag.*, 1986, **133**, pp. 341–350
8 COLLIN, R. E.: 'Field theory of guided waves' (McGraw-Hill, New York, 1960), pp. 85, 174–179, 198–209, Chap. 6
9 LAX, B. K. J., BUTTON, K. J., and ROTH, L. M.: 'Ferrite phase shifters in rectangular waveguide', *J. Appl. Phys.*, 1954, **25**, pp. 1413–1421
10 UHER, J., ARNDT, F., and BORNEMANN, J.: 'Dielectric slab matched ferrite gyrator', *Electron. Lett.*, 1987, **23**, pp. 278–279
11 ARNDT, F., BORNEMANN, J., and VAHLDIECK, R.: 'Design of multisection impedance-matched dielectric-slab filled waveguide phase shifter', *IEEE Trans.*, 1984, **MTT-32**, pp. 34–38

IMPROVED SCHEDULING OF TRAFFIC FOR A HIGH-SPEED SLOTTED RING

Indexing terms: Telecommunications, Communications networks

We describe a new scheduling protocol, designed to work efficiently at very high speeds over large distances and adaptable to support arbitrary mixtures of different types of traffic. While the concept may be applied to different types of LANs and MANs, we explore it here in the context of a slotted ring with packet reuse.

Introduction: The cost of high-capacity fibre-optic communications systems and the cost of ever more complex VLSI chips will continue their steady fall, at least for the next few years. The resulting availability of cheap communications and processing provides a stimulus to explore viable alternatives to today's communications architectures. The application of optical communications to long-distance transmission where large traffic cross-sections are common is obvious and proceeding apace. Within local distribution, however, the challenge is to find ways of cost-effectively sharing the very large capacitances among many users (so-called multiple-access communications), so as to spread the cost of a system over a group of users. There have been many interesting proposals to do this, among them Fasnet,[1] Magnet,[2] FDDI[3] and Orwell.[4] Each differs in the precise way in which they schedule traffic for transmission on the medium. All of them exercise control, and obtain fairness by operating in cycles. Cycles are frequently separated by an intercycle gap equal to the round-trip propagation time of the medium. This intercycle gap is used to establish that all stations have had an opportunity to transmit in a given cycle and cause the start of a new cycle.

We describe here a new protocol called load-controlled scheduling of traffic, or LOCOST for short. The concept is particularly simple and may be applied to virtually any type of network. The first application was to a network configuration of the Fasnet type.† Here we describe our simulation results of applying LOCOST to a slotted ring with destination release of the token, i.e. similar to Orwell.[4] We compare the performance of LOCOST with Orwell.

Table 1 SUMMARY OF CONTROL ALGORITHM APPLIED INDEPENDENTLY AT EACH STATION

(*a*) Count busy packets on line over period P:

$$\text{count} = Y$$

(*b*) Calculate gain factor from value of Y:

$$g = f(Y)$$

(*c*) Calculate packet allowance X:

$$X_i = gX_{i-1}$$

for the ith period

(*d*) Incorporate decay factor a:

$$X_i = a(X_i - X_t) + X_t$$

to provide convergence of X_i at each station

Description of LOCOST: A station wishing to transmit packets measures the traffic on the ring for a given period, say 200 slots. By comparing this measurement Y with the desired number of packets Y_t in the period, the station determines how many packets it may send during the next measurement period. This packet allowance X_i for the ith period is based on the allowance used in the previous period X_{i-1}. The control algorithm is summarised in Table 1 and Fig. 1.

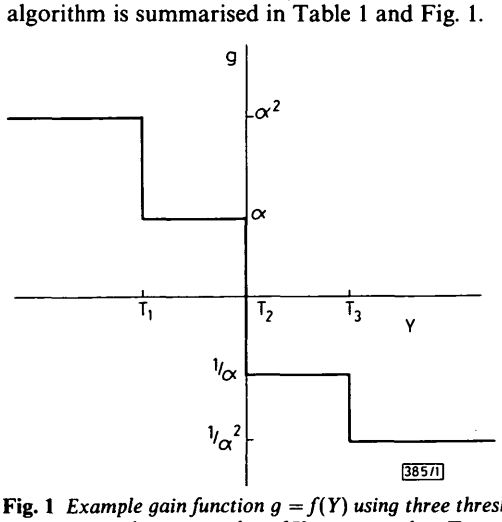

Fig. 1 *Example gain function $g = f(Y)$ using three thresholds T_1, T_2 and T_3, where Y_t, the target value of Y, is set equal to T_2*

Application to a slotted ring: We assume an optical ring operating at 1 Gbit/s, with 1000 bit slots, of length of 10 km. These figures imply that each slot is 1 μs long and that approximately 50 slots will be travelling around the ring. We present

† LIMB, J. O.: 'Load controlled scheduling of traffic for high-speed LANs and MANs', submitted to *IEEE Trans.*, COM